Journal of High School Science

Applying Hodgkin-Huxley model simulations to identify effects of Parkinson's Disease on the action potentials of hippocampal neurons

Han B

Submitted: June 13, 2024, Revised: version 1, July 29, 2024
Accepted: July 30, 2024

Abstract

The neurodegenerative effects of Parkinson's disease have been linked to physiological abnormalities at a cellular level, notably the intracellular accumulation of misfolded α-synuclein. This paper investigated how these cellular abnormalities affect hippocampal neurons' ability to generate action potentials, a process that plays a central role in the transmission of information and higher-order cognitive capabilities. In order to do so, lab recordings were collected from the hippocampal neurons of mice with and without Parkinson's disease. During each recording, a 0.2-second period of no applied current was followed by 0.2 seconds of a 100 mA applied current and another 0.2 seconds of no applied current. The applied current artificially raised the membrane potential past the activation threshold, causing it to generate multiple consecutive action potentials. This data was then fitted to simulations of the Hodgkin-Huxley model in MATLAB by manipulating seven parameters (maximum sodium conductance, maximum potassium conductance, small conductance calcium-activated potassium channel conductance, T-type calcium channel conductance, L-type calcium channel conductance, A-type potassium conductance, and membrane capacitance), the values of which were then collected and quantitatively analyzed to confirm a statistically significant disparity. Results confirmed a statistically significant relationship between Parkinson's and the downregulation of voltage-gated sodium channels, the upregulation of voltage-gated potassium channels, and a reduction in membrane capacitance. These results suggested an increase in neuronal noise and weaker action potentials as well as a decrease in size among hippocampal neurons with Parkinson's disease, providing insight into how the condition impairs neurotransmission. Furthermore, neurons with Parkinson's displayed 0.5 to 0.7 times the percent relative standard deviation (%RSDs) for various channel conductances compared to the control, suggesting a relation between lower heterogeneity of action potentials and Parkinson's disease. This aligns with theories of matrix imbalances of neurotransmitters being causative of Parkinson's disease.

Keywords

Computational biology, Bioinformatics, Computational neuroscience, Parkinson's Disease, Hodgkin-Huxley model, Voltage-Gated ion channel, Hippocampal neurons, Neurotransmission, Transmembrane potential, Synuclein

Brandon Jungwoo Han, Chadwick International School, 45 Art center-daero 97beon-gil, Yeonsu-gu, Incheon, Korea. brandon.jungwoo.han@gmail.com

Introduction

It has long been understood that a primary mechanism through which neurons transmit information and carry out physiological processes is through action potentials, also known as nerve impulses. Neurons typically sustain a negative transmembrane potential (known as the resting potential) through the regulation of ion movement across the neuronal membrane, primarily through the control of potassium, sodium, and calcium ions. In a state of resting potential, the cytosol is elevated in potassium whereas the extracellular fluid has high concentrations of sodium, allowing the inside of the cell to maintain a slight negative charge (1). The cell membrane also has several potassium channels activated whereas most sodium channels are inactive, resulting in a high potassium conductance (g_K) and low sodium conductance (g_{Na}). Due to this selective permeability, the resting potential is situated near the equilibrium potential of potassium (E_K), i.e. at ~ -70 mV (2).

An action potential is a very brief, temporary reversal of the polarity of the membrane potential, caused by an intricate series of activating and deactivating transmembrane proteins that dictate the movement of ions into and out of the neuron. From the point of initiation, the impulse propagates down the axon of the neuron, causing a major intracellular chemical shift that can induce a corresponding response from nearby neurons (1). To briefly describe this mechanism, the action potential can be distinguished into a depolarization and repolarization phase. Depolarization occurs when fluctuations in potassium and sodium concentrations cause the membrane potential to surpass a certain threshold, at which time voltage-gated sodium channels activate at once. This causes a significant, temporary increase in sodium conductance, as sodium ions rapidly move down the electrochemical gradient into the cell. The spontaneous ion movement causes a spike in membrane potential, wherein it approaches the equilibrium potential of sodium (E_{Na}), before entering repolarization.

During repolarization, the voltage-gated sodium channels deactivate, causing potassium conductance to surpass sodium conductance once again. The newly established positive charge inside the cell creates a strong electrochemical gradient that facilitates the movement of K ions out of the cell, causing the polarity of the inside of the cell to rapidly drop back near the equilibrium potential of potassium (E_K). Once repolarization is complete, sodium-potassium pumps are utilized to reinstate the chemical gradient and prepare the neuron for another action potential.

It is important to note here that the voltage-gated sodium channels cannot reactivate until the membrane potential falls below the activation threshold. This results in a short period following repolarization known as the absolute refractory period, during which the neuron is incapable of firing a nerve impulse. The absolute refractory period is followed by the relative refractory period, where the neuron is still in its regenerative state but is capable of firing another action potential at a higher activation threshold.

Parkinson's disease is a chronic neurodegenerative disorder that causes difficulty with coordination and balance, as well as many typical dementia symptoms such as depression and impairment of major cognitive faculties (3). Previous research has established a clear connection between Parkinson's and Lewy Body Dementia, a type of dementia caused by an abnormal accumulation of intracellular α-synuclein protein clumps known as Lewy bodies. Thus, it is well

established that Parkinson's disease is caused by, or at least correlated to, disruptions of biological mechanisms at the cellular level.

This paper aims to observe the effects of Parkinson's disease on the action potential mechanisms of hippocampal neurons. More specifically, it aims to find which transmembrane channels are affected by the disease, and the qualitative effect it would have on the neuron's ability to generate nerve impulses. This was done through a quantitative comparison of membrane potential data from the hippocampal neurons of mice with and without Parkinson's disease, collected from a lab in the American University of Beirut (AUB).

The paper begins by providing an overview of the Hodgkin-Huxley model, the computational framework used to extract information on channel conductances from membrane potential data. The model was then coded into MATLAB, and several simulations were performed to qualitatively observe the effects of various parameters on the neuron's action potential. Seven parameters were manipulated: maximum sodium conductance (g_{Na}), maximum potassium conductance (g_K), small conductance calcium-activated potassium (SK) channel conductance (g_{SK}), T-type calcium channel conductance (g_T), L-type calcium channel conductance (g_L), A-type potassium conductance (g_A) and capacitance (C).

A patch clamp was used to collect information on the membrane potentials of eleven hippocampal neurons, six without Parkinson's and five with Parkinson's. The Hodgkin Huxley model simulation was then calibrated to the data by manipulating the seven aforementioned parameters. This allowed for the values of the seven parameters to be obtained for all eleven neurons, after which a statistical analysis was performed to determine which parameters and channel conductances demonstrated a statistically significant disparity.

Please note that the data used in this paper was not collected by the author, but received from the Daou Lab in the American University of Beirut (AUB).

Materials and Methods

The Hodgkin-Huxley Model

The Hodgkin-Huxley model is essentially a quantification of the various biological processes previously described. The model is based on the principle that a cell is analogous to a circuit; similar to a capacitor, the cell membrane can store charge between both sides, while channel proteins act as resistors, allowing current to flow through (4). This analogy permits the application of many well-established formulas used in currents onto cell potential. The Hodgkin-Huxley model primarily uses the following two relationships:

$$I(t) = g \cdot V(t) \qquad (1)$$

$$\frac{d}{dt}V(t) = \frac{d}{dt}\frac{Q(t)}{C} = \frac{I_C(t)}{C} \Rightarrow C\frac{dV}{dt} = I_C(t) \qquad (2)$$

Where I_C represents the current that is charging the capacitor. The flow of each individual ion as well as the current charging the capacitor represent separate currents in the circuit, which must add up to the applied current. Thus, equation 3 follows. Equations 4 and 5 follow from Hodgkin and Huxley's assumption that each ionic current obeys Ohm's law.

$$I_{app} = I_C(t) + I_{ion}(t) \quad (3)$$

$$I_{ion} = \Sigma G_i(V_m, t)(V_m - E_i) \quad (4)$$

$$\Rightarrow C\frac{dV}{dt} = I_C(t) = I_{app} - \Sigma G_i(V_m, t)(V_m - E_i) \quad (5)$$

V_m denotes the membrane potential, E_i represents the equilibrium potential of an ion, and $G_i(V_m, t)$ represents the voltage-dependent membrane conductance for each ion, which is determined by the activity of various transmembrane channel proteins (5). Equation 5 serves as the base, most fundamental equation for all variations of the Hodgkin-Huxley model. The details regarding $G_i(V_m, t)$ for each ionic current needed consideration. In the version of the Hodgkin-Huxley model used for this paper, there were six total channels that were manipulated during calibration. These included potassium channels, voltage-gated sodium channels, small-conductance calcium-activated potassium (SK) channels, T-type calcium channels, A-type potassium channels, and L-type calcium channels.

Bower et. al. communicated that, according to the Hodgkin-Huxley model, the activity of an ion channel depends on the positioning of various protein domains, and all the relevant domains must be in the permissive position in order for a protein channel to open. In other words, even if one domain is in an inactivating position, the ion channel cannot activate. Therefore, the open probability of a gate is strongly dependent on the behavior of these domains (or particles) (6). The behavior of each individual particle can be thought of as a first order chemical reaction between a permissive state and inactivating state. Two parameters, known as transition rate constants, dictate how the particle moves between the two positions (6). The first transition rate constant (denoted as α) represents the proportion of particles in the inactivating position that transition to the permissive position per second. Similarly, the second transition rate constant (referred to as β) represents the proportion of particles in the permissive position that transition to an inactivating position per second (6).

From these definitions, if n is the proportion of particles in the permissive state, equation 6 is obtained.

$$\frac{dn}{dt} = \alpha(1 - n) - \beta n \quad (6)$$

Based on their data, Huxley and Hodgkin concluded that the activation of potassium channels depended on the position of four n-particles. Thus, the proportion of open potassium channels = $n(t)^4$, assuming that the behavior of each particle is independent of the others (5). As conductance is proportional to the number of open channels, equation 7 is obtained.

$$G_K(V, t) = g_K n(V)^4 \quad (7)$$

$$\text{where } \frac{dn}{dt} = a_n(V)(1 - n) - \beta_n(V)n \quad (8)$$

and g_K denotes the maximum potassium conductance. Similarly, the activation of sodium channels depended on three m-particles and one h-particle (5). Thus, equation 9 is obtained.

$$G_{Na}(V,t) = g_{Na}m(V)^3h(V) \quad (9)$$

where $\frac{dm}{dt} = \alpha_m(V)(1-m) - \beta_m(V)m$ (10)

and $\frac{dh}{dt} = \alpha_h(V)(1-h) - \beta_h(V)h$ (11)

The other three channels can be similarly mathematically modeled, with slight variations in the number and types of particles.

L-type Calcium Channels

L-type calcium channels activate at a very high voltage threshold for relatively long periods of time. They are controlled by the positions of two s-particles (7).

$$I_{Ca-L} = g_{Ca-L}s(V)^2(V - E_{Ca}) \quad (12)$$

T-type Calcium Channels

T-type calcium channels activate at low voltages and become inactive during hyperpolarization. These channels control the movement of calcium after the action potential is reached, and they depend on the positioning of 3 a-particles and 2 b-particles (7). The L and T-type calcium channels dictate the behavior of calcium through the cell membrane, which can be represented by equation 14.

$$I_{Ca-T} = g_{Ca-T}a(V)^3b(V)^2(V - E_{Ca}) \quad (13)$$

$$\frac{dCa}{dt} = -\delta(I_{Ca-L} + I_{Ca-T}) + \theta([Ca] - 0.1) \quad (14)$$

SK Channels (Calcium-dependent Potassium Channels)

SK channels are activated by an increase in intracellular calcium and limit the firing frequency of action potentials (8). These are modeled by equations 15 and 16. A-type potassium channels were also included in the model (equation 17, l is a constant).

$$I_{SK} = g_{SK}k_\infty[Ca](V - E_K) \quad (15)$$

$$k_\infty = \frac{[Ca]^2}{[Ca]^2+\sigma^2} \quad (16)$$

$$I_{A-typePotassium} = gA \cdot l \cdot (V_m - V_K) \quad (17)$$

The objective of this investigation was to calibrate the Hodgkin-Huxley model to lab recordings of membrane potentials by manipulating the following seven parameters: maximum sodium conductance (g_{Na}), maximum potassium conductance (g_K), small conductance calcium-activated potassium (SK) channel conductance (g_{SK}), T-type calcium channel conductance (g_T), L-type calcium channel conductance (g_L), A-type potassium conductance (g_A) and capacitance (C). In order to successfully do so, simulations were performed with variations in these parameters to observe their effect on the action potential.

Model simulations

Initial experimentation with the model commenced by modifying various parameters which control the behavior of action potentials. Qualitative observations were made regarding the effect of these parameter modifications on the neuron's behavior under an applied current. In all simulations, a 0.2-second period of no applied current was followed by 0.2 seconds of an applied positive 100mA current into the cell, as well as 0.2 additional seconds of no applied current.

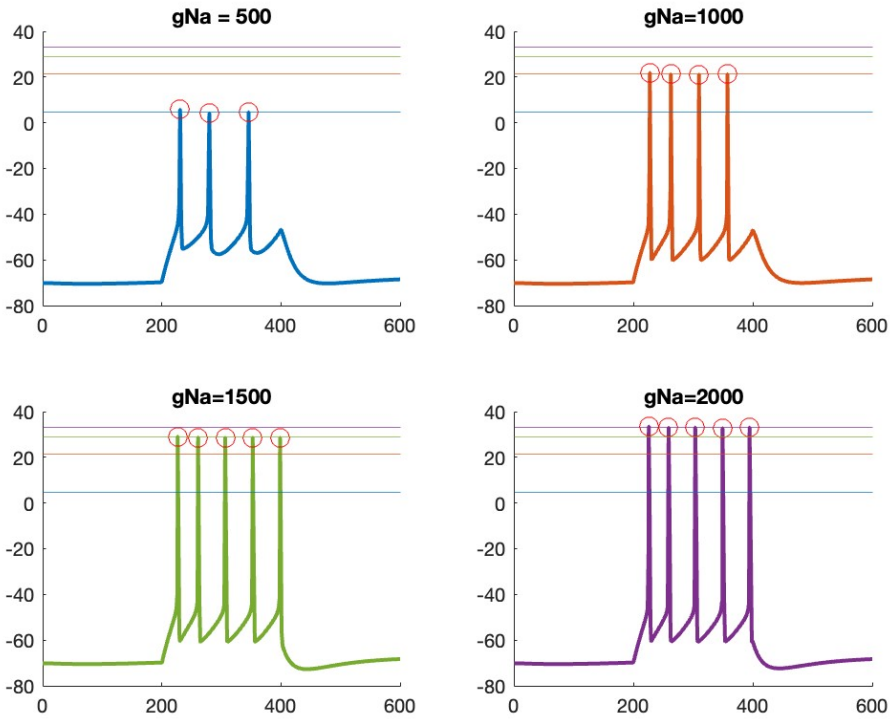

Figure 1. Simulation results with maximum sodium conductance set as 500 (top left), 1000 (top right), 1500 (bottom left), and 2000 (bottom right) $cS(0.01\Omega^{-1}, centiSiemens)$. The horizontal bars, which are in the four colors blue ($gNa = 500$), orange ($gNa = 1000$), green ($gNa = 1500$) and purple ($gNa = 2000$) denote the average peak height for their corresponding graphs.

As shown in Figure 1, the maximum sodium conductance g_{Na} demonstrated considerable impact on the frequency of action potentials, as the number of spikes increased from 3 to 5. This outcome was expected, since higher sodium conductance implies faster depolarization and thus an overall reduction of the duration of each action potential. Furthermore, this parameter significantly affected the amplitude of the action potential. When the maximum sodium conductance was set to 1000 cS, the spike peaked at +20 mV. However, when the

maximum sodium conductance was set to 1500 cS the peak reached +30 mV. Thus, there was a positive correlation between sodium conductance and spike height. This relationship is visually confirmed by the increasing height of the horizontal bars as sodium conductance increases. The positive correlation between peak height and sodium conductance aligns with our understanding of the biological processes behind action potentials. Sodium ions primarily drive the depolarization that occurs when a neuron surpasses its activation threshold, as it is the rapid increase in intracellular sodium that causes membrane potential to spike. Thus, a stronger sodium conductance resulting in stronger sodium current leads to a higher peak membrane potential, approaching closer to the equilibrium potential of sodium.

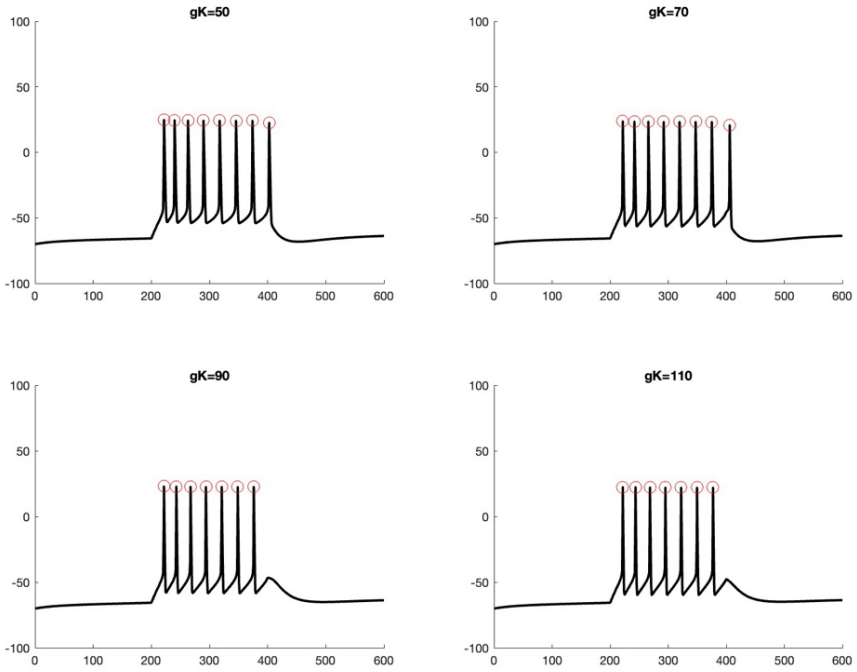

Figure 2. Simulation results with maximum potassium conductance set as 50 (top left), 70 (top right), 90 (bottom left), and 110 (bottom right) $cS(0.01\Omega^{-1})$.

The maximum potassium conductance g_K had a major influence over the refractory period of the neuron, as potassium movement plays a role in the repolarization and post hyperpolarization phases. Specifically, the decrease in intracellular potassium was responsible for driving the membrane potential back down after reaching the action potential. Therefore, an increase in maximum potassium conductance and thus potassium current caused the membrane potential to decrease more rapidly and further below the activation threshold, extending the refractory period during which the membrane potential stabilized and reached a point where a subsequent action potential was possible. This relationship is evident in Figure 2, where an increase in potassium conductance corresponds to a lower frequency of action potentials, as the number of peaks decreases from 8 to 7. Furthermore, the average minimum membrane potential during the hyperpolarization phase decreased from -59.1 mV to -64.6 mV as g_K increased from 50 to 110 cS, while the time between the second and third spikes decreased from 33.3ms to 24.9 ms; both indicative of a steeper and extended

hyperpolarization phase as a result of the membrane potential dropping further below the activation threshold, as potassium conductance increased. Thus, there was a negative correlation between firing frequency and potassium conductance. On the other hand, there was no noticeable change in the peak membrane potential, as potassium plays a relatively minor role in the depolarization phase.

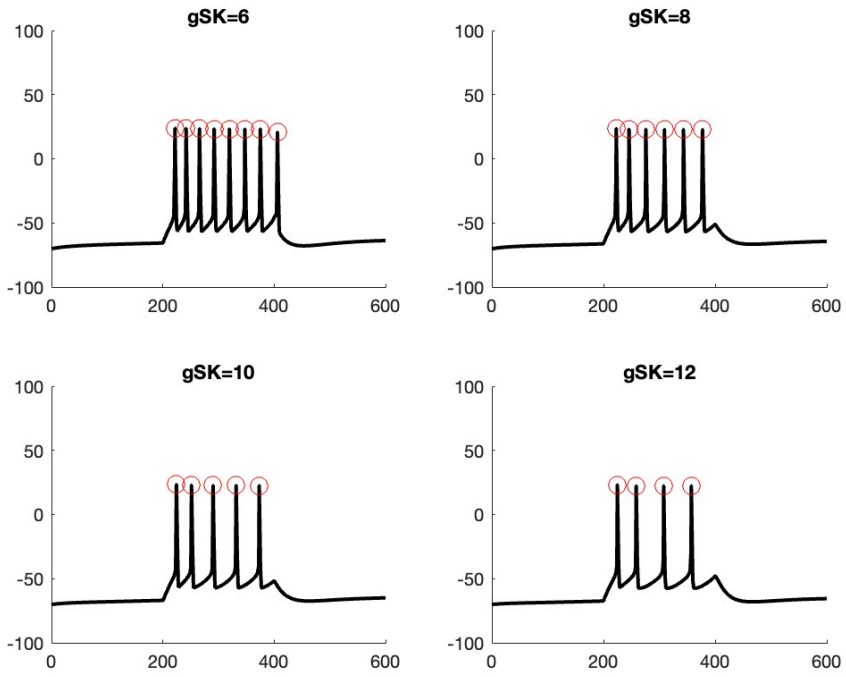

Figure 3. Simulation results with SK conductance set as 6 (top left), 8 (top right), 10 (bottom left), and 12 (bottom right) Ω^{-1}.

SK channels play a critical role in limiting the firing frequency of neurons. This effect is achieved through the gradual leakage of potassium ions out of the cell through SK channels during post hyperpolarization. As SK channels activate in response to an influx of calcium during the overshoot, a current of potassium ions out of the cell forms through these newly activated channels. This lowers the membrane potential closer to the equilibrium potential of potassium and delays the neuron's recovery back to its resting state, extending its refractory period (8). The significance of this mechanism can be observed in the simulations in Figure 3, where the frequency of action potentials decreased from 8 to 5 due to an increase in SK conductance by 6 Ω^{-1}. In other words, the stronger potassium current out of the cell through SK channels during the undershoot extended the refractory period and regulated the firing rate of the neurons (8).

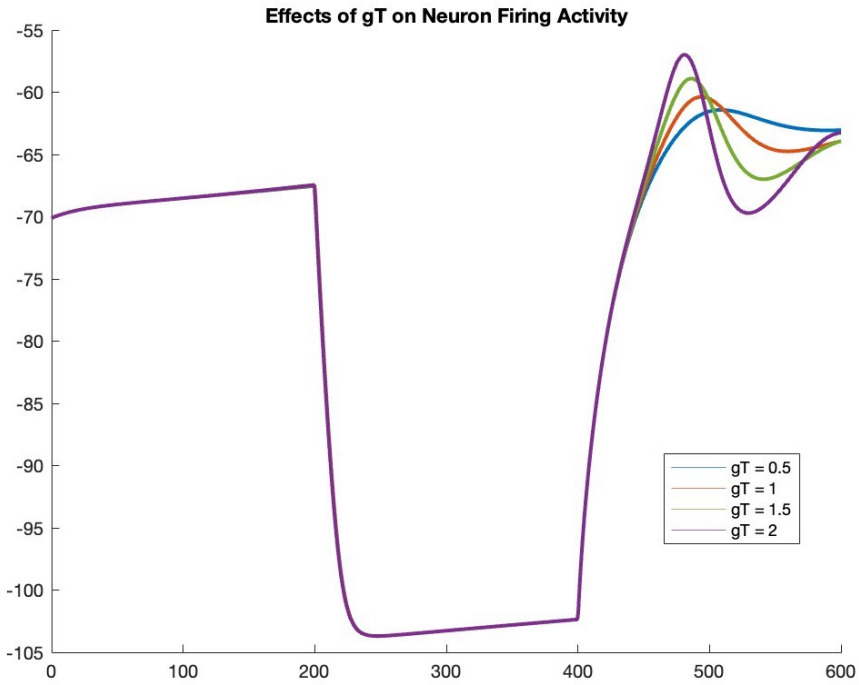

Figure 4. Simulation results with T conductance set as 0.5 (blue), 1 (orange), 1.5 (green), and 2 (purple) Ω^{-1}. For these simulations, a negative current was applied onto the model in order to better visualize the hyperpolarization of the neuron.

T-type calcium channels activate during depolarization at relatively low voltages with an activation threshold of -55 mV, similar to that of voltage-gated sodium channels. Within this range of membrane potentials, there exists a large force driving calcium ions into the cell. Consequently, the activation of T-type calcium channels causes a significant increase in intracellular calcium concentrations. This, in turn, facilitates further depolarization above the -55 mV point, playing a critical role in calcium signaling interactions with other proteins such as SK channels.

This function of the T-type channel can be clearly observed *via* the simulations in Figure 4. From 0 to 450 ms, there were no noticeable effects of T-type calcium conductance on the membrane potential, as the membrane potential remained well below the inactivation threshold of -55 mV. However, as the neuron rebounded back to resting potential, a higher T-type conductance caused a much more pronounced overshoot, driven by the stronger intracellular calcium current that elevated the membrane potential further.

L-type calcium channels activate at high voltages, increasing intracellular calcium concentrations and facilitating the activation of SK channels during hyperpolarization. Thus, an increase in L-type calcium conductance results in a decrease in firing frequency due to the increased activity of SK channels, which limit the firing frequency of neurons. This effect was evident in the simulations presented in Figure 5, where a demonstrable reduction in action potentials occurred, decreasing from 8 to 5 as a result of an increase in L-type conductance from 10 to 40 Ω^{-1}.

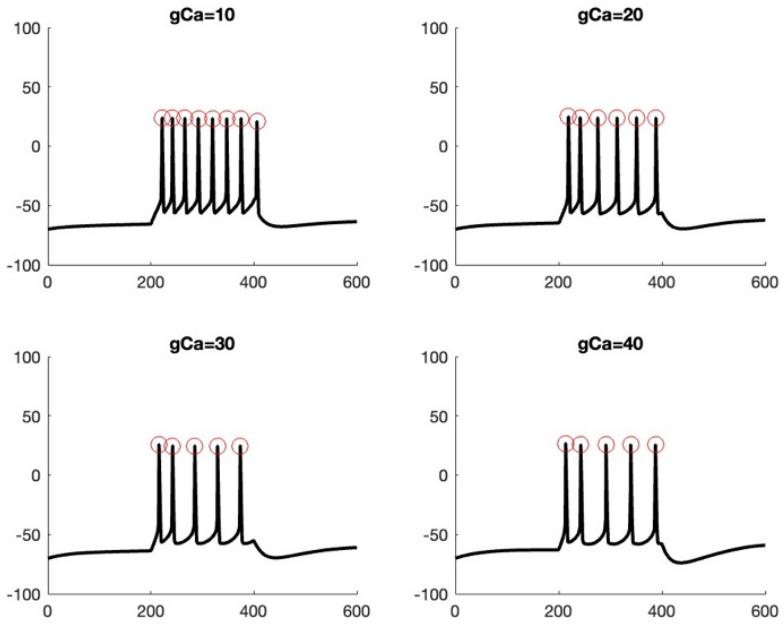

Figure 5. Simulation results with L-type calcium conductance set as 10 (top left), 20 (top right), 30 (bottom left), and 40 (bottom right) Ω^{-1}.

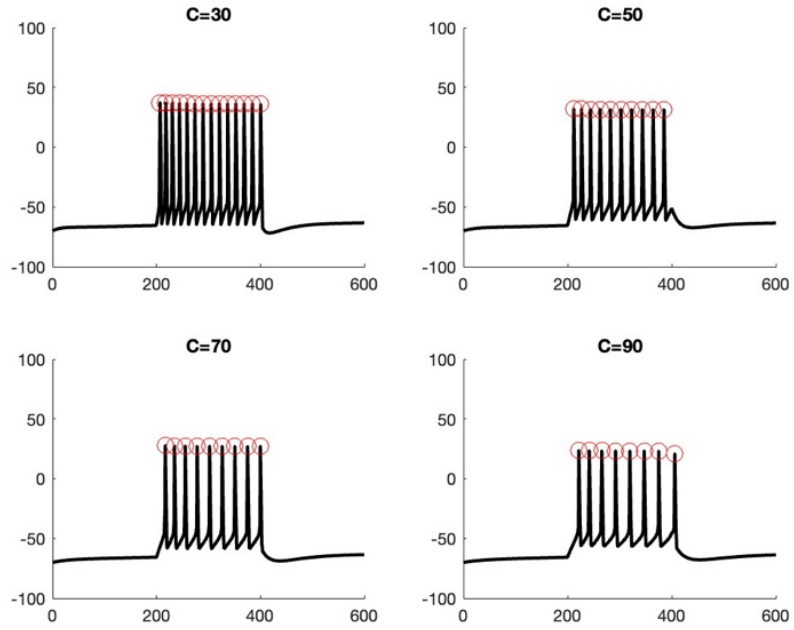

Figure 6. Simulation results with Capacitance set to 30 (top left), 50 (top right), 70 (bottom left), and 90 (bottom right) pF.

The derivative of membrane potential with respect to time is inversely proportional to capacitance. Thus, an increase in capacitance leads to a weaker response in membrane potential in response to external stimuli. In the simulations shown in Figure 6, this was reflected in the lower action potentials. At a capacitance of 30pF, the action potential's peaked near +40 mV; when the capacitance increased to 90pF, the action potential's peak was near +20 mV. Furthermore, an additional effect of higher capacitance is a slower

repolarization and hyperpolarization due to the slower changes in membrane potential, leading to an extended refractory period and thus lower firing frequency. This can also be observed in the simulations in Figure 6, as the number of peaks decreased from 14 to 8 due to an increase in capacitance.

Membrane potential data collection

The whole-cell patch clamp method was used to collect data on the neuron membrane potential. To briefly describe the technique, a pipette was used to make contact with a small patch of the neuronal membrane. Briefly applying strong suction ruptured the membrane and allowed the pipette to be in electrical continuity with the cytoplasm. This arrangement allowed for accurate measurements of the electrical potential difference of the cell's interior and external environment, which is its membrane potential. In order to allow for a comparison between neurons with and without Parkinson's disease, measurements were obtained from six hippocampal neurons from mice without Parkinson's disease and five hippocampal neurons from mice with Parkinson's dementia.

Model calibration to recorded data

The Hodgkin-Huxley model was fitted to the lab data through an iterative process. Each parameter was continuously shifted by intervals between 0.05 and 5 and the parameter value that returned the closest simulation results to the data was found. This process was repeated for each parameter several times until a simulation result was obtained that satisfactorily matched the lab data. Factors that were considered when judging whether a simulation result was appropriately calibrated were the time and height of spikes, resting potentials of the neuron, and duration of refractory periods between successive action potentials.

Results

The observations presented above regarding the effects that changes in parameters had on the neuron were used to calibrate the model with various membrane potential recordings from these neurons.

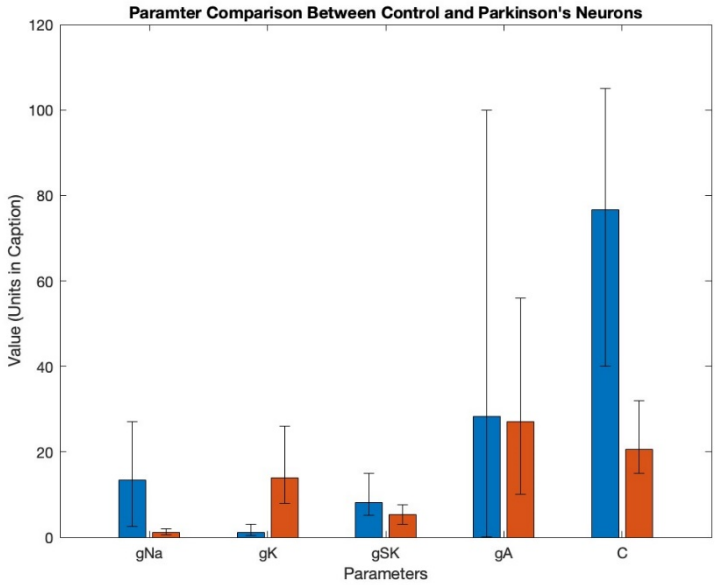

Figure 7. A bar graph comparing the average channel conductance of neurons in the control group (blue) versus hippocampal neurons with Parkinson's disease (red). Error bars denote the maximum and minimum values for each parameter. The units for gNa and gK are $0.01S$ while for gSK and gA the units are $1S$ and for capacitance the unit is picofarads.

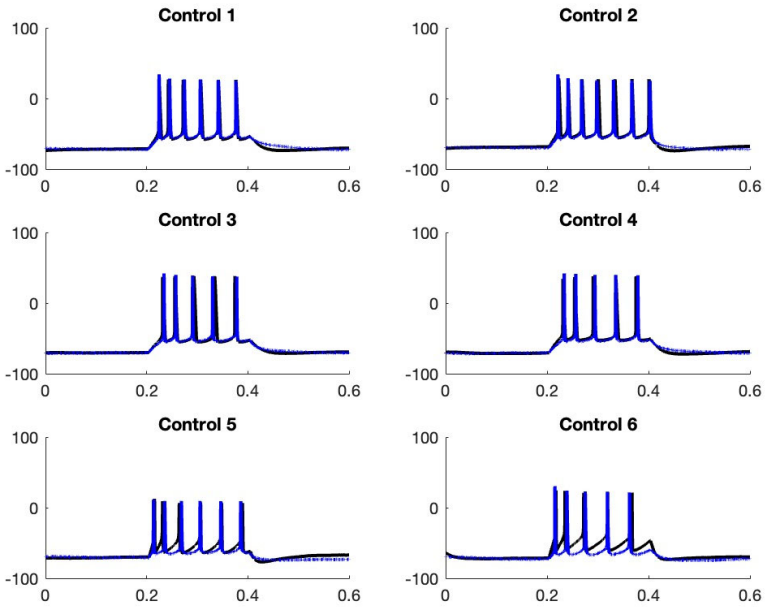

Figure 8. A series of diagrams showing the simulated membrane potential (black) plotted against the lab data (blue). As shown above, all six neurons were fitted to a reasonable degree of accuracy, with the frequency of action potentials and spike height being almost identical between the two.

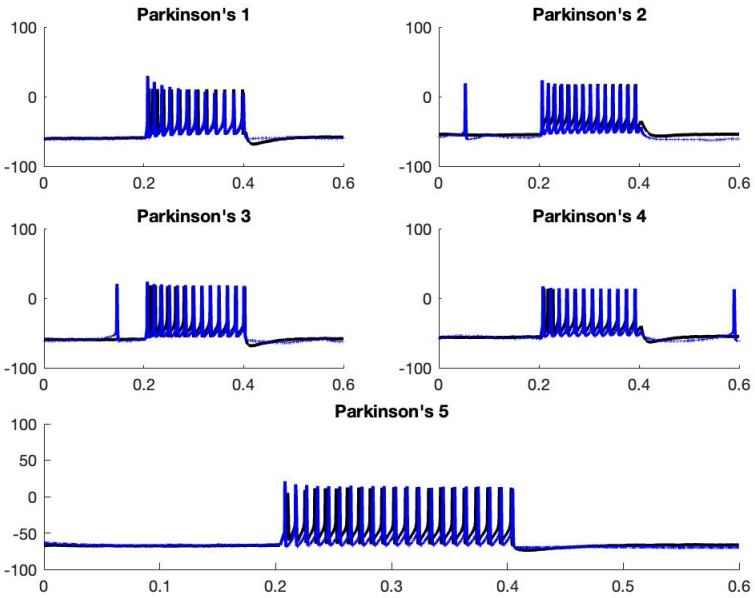

Figure 9. A series of diagrams showing the simulated membrane potential (black) plotted against the lab data (blue). Similar to the neurons in the control group, all five neurons were plotted to a reasonable degree of accuracy, with additional emphasis being placed on firing frequency, spike height, and resting potential.

Table 1. A table showing the parameters input into the simulated neuron in order to obtain the fits displayed in figures 8 and 9.

	Channel Conductance (Units: 0.01S for gNa and gK, 1S for gSK and gA)				Capacitance (pF)
	gNa	gK	gSK	gA	
Control 1	1300	50	5.1	10	90
Control 2	1200	55	5.45	10	90
Control 3	2700	60	5.95	50	105
Control 4	2200	45	5.3	100	90
Control 5	250	200	11.7	0.01	45
Control 6	370	300	15	0.01	40
Control Average	1336.67	118.33	8.08	28.34	76.67
Parkinson's 1	70	900	6	10	20
Parkinson's 2	200	1800	3	56	32
Parkinson's 3	90	800	7.7	14	15
Parkinson's 4	80	2600	6.07	15	20
Parkinson's 5	150	900	4	40	16
Parkinson's Average	118	1400	5.35	27	20.6

As shown in Figure 7, there were demonstrable disparities in the parameter values between hippocampal neurons in the control group and neurons with Parkinson's. A two-sample t-test was run to confirm that such a disparity existed, using the conventional level of significance $\alpha = 0.05$. The results appear in Table 2.

Table 2. A table showing results of a two-sample t test between neurons in the control group ('Control') and neurons with Parkinson's ('Dementia'). The parameters gNa, gK, and C showed a statistically significant disparity with P-values of 0.0278, 0.0211, and 0.0031, respectively. The parameters gSK and gA, meanwhile, failed to reach the threshold of statistical significance.

	Control Mean	Dementia Mean	Control SD	Dementia SD	T value	P value	Statistically Significant?
gNa	1336.667	118	973.584	55.408	3.06	0.0278	Yes
gK	118.333	1400	106.896	784.219	-3.626	0.0211	Yes
gSK	8.083	5.354	4.22	1.858	1.427	0.196	No
gA	28.337	27	39.704	20.075	0.072	0.9443	No
Capacitance	76.667	20.6	27.142	6.768	4.881	0.0031	Yes

As shown in Table 2, the computational analysis indicated that there was a statistically significant difference in the activation of sodium channels, potassium channels, and the conductance. More specifically, in neurons affected by Parkinson's disease, voltage-gated sodium channels were downregulated, while voltage-gated potassium channels were upregulated, and capacitance was significantly lower than normal.

Table 3. A table of % relative standard deviation (RSD) values for parameters in neurons of the control and Parkinson's groups. The parameters gNa, gK, gSK, and gA all show significantly lower %RSD values in the Parkinson's group, with the %RSD values of the Parkinson's group ranging from 0.5 to 0.7 times that of the control group (except for capacitance).

	Control %RSD	Dementia %RSD	Dementia/Control %RSD Ratio
g_{Na}	72.8	47.0	0.6
g_K	90.3	56.0	0.6
g_{SK}	52.2	34.7	0.7
g_A	140.1	74.4	0.5
Capacitance	35.4	32.9	0.9

Discussion

From a physiological perspective, the downregulation of voltage-gated sodium channels in neurons affected by Parkinson's provides a justification for many of its neurodegenerative effects. As previously described, the influx of sodium through these channels during depolarization plays a major role in reversing the membrane polarity close to the equilibrium potential of sodium (2). If there is a downregulation in these channels, the depolarizing mechanism would be significantly impaired, reducing the amplitude of the neuron's membrane potentials. This can be observed in the lab recordings from figures 8 and 9; whereas neurons in the control group reached membrane potentials of 25-30 mV, the neurons with Parkinson's failed to reach > 20 mV. This decrease in maximum membrane potentials was also largely due to the lower baseline potential of neurons with Parkinson's compared to those of the control group; whereas the potential of neurons in Figure 8 remained above the resting potential between nerve impulses, the potential of neurons in Figure 9 decreased back to the resting potential (baseline) during refractory periods. This is due to the upregulation of voltage-gated potassium channels, as the larger potassium outcurrent caused membrane potential to drop much further while sodium channels recovered for providing the subsequent action potential. A weaker action potential impedes neuron-to-neuron communication, as action potentials play a signaling role between neurons and trigger many mechanisms involved in neurotransmission (9). Thus, smaller action potential lead to slower response times in neural circuits and impede the brain's cognitive capabilities.

Spontaneous neural activity has been associated with fluctuations in potassium concentrations (14), and thus the upregulation of potassium channels and greater potassium currents may make the membrane potential more prone to random fluctuations. That is, the upregulation of potassium channels cause higher natural fluctuations in membrane potential, which may be responsible for the spontaneous action potentials that occurred without any applied current in neurons with Parkinson's, as observed in panels 2, 3, and 4 in figure 9. Biologically, the random activation of action potentials without any external stimuli contributes to an increase in neuronal noise, which impedes the brain's ability to process information and perform fundamental physiological processes (10). The analyses above of the results aligned with many common symptoms of Parkinson's disease. Symptoms such as changes in memory and difficulty interpreting visual information can all be attributed to an increase in neural noise and impairment of neurotransmission that limit the brain's ability to process information.

Furthermore, the statistical analysis indicated a significant decrease in membrane capacitance associated with Parkinson's disease. As membrane capacitance is highly correlated with cell size (15), this suggested that the size of hippocampal neurons in the brain of mice with Parkinson's dementia decreased. A possible interpretation could be that the decrease in the size of hippocampal neurons inhibited their ability to form connections with neighboring cells, impeding information processing and causing Parkinson's neurodegenerative symptoms. An alternative explanation would be that unregulated neuronal apoptosis occurred in the hippocampus among neurons with Parkinson's disease, since a hallmark of neuronal apoptosis is a decrease in cell size before death (11).

Although tests failed to demonstrate a statistically significant difference, the results also suggested that a decrease in the conductance of SK channels occurred among neurons with Parkinson's disease. SK channels are a type of calcium-activated potassium channels that play a role in regulating the refractory period of the neuron. During post hyperpolarization, the influx of calcium ions causes SK channels to activate, leading to a transiently high potassium membrane permeability. This amplifies the potassium current outcurrent, causing membrane potential to drop and delaying the neuron's recovery back to resting potential (12). A downregulation of small conductance calcium-activated potassium channels impedes this mechanism, effectively debilitating the neuron's ability to regulate the frequency of action potentials. This effect can be observed in the lab recordings presented in figures 8 and 9. Neurons in the control group produced no more than 7 action potentials in the span of 200 milliseconds, whereas neurons with Parkinson's disease produced sometimes > 20 action potentials in the same time period. Physiologically, this narrative aligns with many common symptoms of Parkinson's. The frequency of action potentials is controlled by neurons in order to encode information about the stimulus (13). Thus, not being able to effectively control firing rate interferes with the brain's sensory processing, as discriminating between sensory inputs becomes a much more difficult task. This phenomenon may also justify difficulty with learning and memory, as synaptic plasticity, a process involved in the formation of new memories and skills, involves changes in firing rates among particular types of neurons.

Apart from differences in the absolute values of individual parameters, a more macroscopic trend that was observed between neurons in the control and Parkinson's groups was significantly lower %RSD values for the parameters g_{Na}, g_K, g_{SK}, and g_A in the Parkinson's group (shown in table 3). Prior publications have suggested that manifestations of Parkinson's disease are caused by matrix imbalances of neurotransmitters (16). It is possible that this matrix imbalance limits the synaptic input diversity of individual neurons, causing lower heterogeneity of channel conductance values and action potentials. These lower variations in channel conductance values may be more influential causes of clinical manifestations of Parkinson's, more so than the absolute values of individual parameters themselves. However, further experimentation would be needed to confirm this relationship.

On a final note, although significant disparities in parameter values between neurons with and without Parkinson's were found, it is difficult to determine which of these parameters had a decisive effect on the behavioral differences between these two groups of neurons. A local

sensitivity analysis of how individual parameters affect action potentials may allow better insight into the most influential factors affecting neurons with Parkinson's.

Conclusion

Hippocampal neurons with Parkinson's Disease exhibited significantly lower membrane capacitance, downregulated sodium channels, and upregulated potassium channels. Furthermore, the data suggested a downregulation of SK channels, although a statistically significant disparity was not confirmed. These physiological abnormalities are in agreement with and provide potential justifications for several observed symptoms of Parkinson's Disease, such as difficulty processing visual information, impeded memory, and slower response times.

Neurons with Parkinson's were also observed to have substantially lower percent relative standard deviation (%RSD) values for channel conductance values compared to those in the control group. This observation is consistent with published literature where manifestations of Parkinson's disease are reported to be caused by matrix imbalances of neurotransmitters. It is possible that this lower %RSD – indicative of lower heterogeneity of channel conductance values and action potentials – may limit the synaptic input diversity of individual neurons and manifest as symptoms of Parkinson's disease. It is difficult to definitively state the effect of this phenomenon on cognitive function, and further research would be needed to confirm this phenomenon.

Additional studies on the up and downregulation of various proteins associated with Parkinson's can facilitate the development of a treatment for the disease. Pharmacologically regulating these proteins to reverse abnormal modifications in their activity may mitigate the condition's neurodegenerative effects. If a causal relationship is identified, such a treatment may prevent the onset of the disease entirely.

Acknowledgements

I would like to thank Dr. Arij Daou for mentoring the writing of this paper. I would also like to thanks Ms. Sophie Phillips for providing feedback during the paper editing stages.

References

1. Barnett M. W., Larkman P. M. The Action Potential. Pract. Neurol. 2007, 7 (3), 192–197. https://www.researchgate.net/publication/6316219_The_action_potential

2. Bear M. F., Connors B. W., Paradiso M. A. Neuroscience: Exploring the Brain, Enhanced fourth edition., Jones & Bartlett Learning: Burlington, MA, 2016.

3. Parkinson's Disease: Causes, Symptoms, and Treatments. National Institute on Aging. https://www.nia.nih.gov/health/parkinsons-disease

4. Siciliano R. The Hodgkin-Huxley Model. https://www.math.mcgill.ca/gantumur/docs/reps/RyanSicilianoHH.pdf

5. Hodgkin A. L., Huxley A. F. A Quantitative Description of Membrane Current and Its Application to Conduction and Excitation. Nerve. J. Physiol. 1952, 117 (4), 500–544. https://doi.org/10.1113/jphysiol.1952.sp004764

6. Bower J. M., Beeman D. The Book of GENESIS: Exploring Realistic Neural Models with the GEneral NEural SImulation System, Biophys J. 1995, 69, 2174-2175. https://www.researchgate.net/profile/D-Beeman/publication/319253881_The_Book_of_GENESIS/links/0deec518c04e871442000000/The-Book-of-GENESIS.pdf

7. Rossier M. F. T-Type Calcium Channel: A Privileged Gate for Calcium Entry and Control of Adrenal Steroidogenesis. Front. Endocrinol. 2016, 7, 43. https://doi.org/10.3389/fendo.2016.00043

8. Bond C. T., Maylie J., Adelman J. P. Small-Conductance Calcium-Activated Potassium Channels. Ann. N. Y. Acad. Sci. 1999, 868, 370–378. https://doi.org/10.1111/j.1749-6632.1999.tb11298.x.

9. Chen I., Lui F. Neuroanatomy, Neuron Action Potential. In StatPearls, StatPearls Publishing: Treasure Island (FL), 2023. https://www.ncbi.nlm.nih.gov/books/NBK546639/

10. Jacobson G., Yaron-Jakoubovitch A., Diba, K., Oz, Y., Koch, C., Segev, I., Yarom, Y. Subthreshold Voltage Noise of Rat Neocortical Pyramidal Neurones. J. Physiol., 2005, 564(1), 125-160. https://doi.org/10.1113/jphysiol.2004.080903

11. Lemkuil B. P., Drummond J. C., Patel P. M. 9 - Central Nervous System Physiology: Cerebrovascular. In Pharmacology and Physiology for Anesthesia (Second Edition), Hemmings, H. C., Egan, T. D., Eds., Elsevier: Philadelphia, 2019, pp 174–192. https://doi.org/10.1016/B978-0-323-48110-6.00009-0

12. Faber E. L., Sah P. Functions of Sk Channels in Central Neurons. Clin. Exp. Pharmacol. Physiol. 2007, 34 (10), 1077–1083. https://doi.org/10.1111/j.1440-1681.2007.04725.x.

13. Deutch A. Y. Chapter 6 - Neurotransmitters. In Fundamental Neuroscience (Fourth Edition), Squire, L. R., Berg, D., Bloom, F. E., du Lac, S., Ghosh, A., Spitzer, N. C., Eds., Academic Press: San Diego, 2013, pp 117–138. https://doi.org/10.1016/B978-0-12-385870-2.00006-8

14. Øyehaug L., Østby I., Lloyd C. M., Omholt S. W., Einevoll G. T. Dependence of Spontaneous Neuronal Firing and Depolarisation Block on Astroglial Membrane Transport Mechanisms. J Comput Neurosci 2012, 32 (1), 147–165. https://doi.org/10.1007/s10827-011-0345-9

15. Major G., Evans J. D., Jack J. J. Solutions for Transients in Arbitrarily Branching Cables: I. Voltage Recording with a Somatic Shunt. Biophysical Journal 1993, 65 (1), 423–449. https://doi.org/10.1016/S0006-3495(93)81037-3

16. Sanchez-Catasus C. A., Bohnen N. I., D'Cruz N., Müller M. L. T. M. Striatal Acetylcholine–Dopamine Imbalance in Parkinson Disease: In Vivo Neuroimaging Study with Dual-Tracer PET and Dopaminergic PET–Informed Correlational Tractography. J Nucl Med 2022, 63 (3), 438–445. https://doi.org/10.2967/jnumed.121.261939